CellPress
PARTNER JOURNAL

Molecular Plant
Research Article

A Post-domestication Mutation, *Dt2*, Triggers Systemic Modification of Divergent and Convergent Pathways Modulating Multiple Agronomic Traits in Soybean

Dajian Zhang[1,2,6], Xutong Wang[1,6], Shuo Li[1,3,6], Chaofan Wang[2], Michael J. Gosney[4], Michael V. Mickelbart[4,5] and Jianxin Ma[1,5,*]

[1]Department of Agronomy, Purdue University, West Lafayette, IN 47907, USA

[2]College of Agronomy, Shandong Agricultural University, Tai'an, Shandong 271018, China

[3]School of Life Sciences, Shandong University, Qingdao, Shandong 266237, China

[4]Department of Botany and Plant Pathology, Purdue University, West Lafayette, IN 47907, USA

[5]Center for Plant Biology, Purdue University, West Lafayette, IN 47907, USA

[6]These authors contributed equally to this article.

***Correspondence: Jianxin Ma (maj@purdue.edu)**

https://doi.org/10.1016/j.molp.2019.05.010

ABSTRACT

The semi-determinate stem growth habit in leguminous crops, similar to the "green revolution" semi-dwarf trait in cereals, is a key plant architecture trait that affects several other traits determining grain yield. In soybean semi-determinacy is modulated by a post-domestication gain-of-function mutation in the gene, *Dt2*, which encodes an MADS-box transcription factor. However, its role in systemic modification of stem growth and other traits is unknown. In this study, we show that Dt2 functions not only as a direct repressor of *Dt1*, which prevents terminal flowering, but also as a direct activator of putative floral integrator/identity genes including *GmSOC1*, *GmAP1*, and *GmFUL*, which likely promote flowering. We also demonstrate that Dt2 functions as a direct repressor of the putative drought-responsive transcription factor gene *GmDREB1D*, and as a direct activator of *GmSPCH* and *GmGRP7*, which are potentially associated with asymmetric division of young epidermal cells and stomatal opening, respectively, and may affect the plant's water-use efficiency (WUE). Intriguingly, Dt2 was found to be a direct activator or repressor of the precursors of eight microRNAs targeting genes potentially associated with meristem maintenance, flowering time, stomatal density, WUE, and/or stress responses. This study thus reveals the molecular basis of pleiotropy associated with plant productivity, adaptability, and environmental resilience.

Key words: abiotic stress, agronomic traits, convergent pathways, stem growth habit, pleiotropy, soybean

Zhang D., Wang X., Li S., Wang C., Gosney M.J., Mickelbart M.V., and Ma J. (2019). A Post-domestication Mutation, *Dt2*, Triggers Systemic Modification of Divergent and Convergent Pathways Modulating Multiple Agronomic Traits in Soybean. Mol. Plant. **12**, 1366–1382.

INTRODUCTION

All flowering plants produce flowers and seeds through the successful transition from vegetative-to-reproductive growth of shoot apices under favorable environmental conditions. While enormous progress has been made toward understanding the molecular basis of flowering (O'Maoiléidigh et al., 2014; Spanudakis and Jackson, 2014), it is still poorly understood why some plants maintain indeterminate stem growth without terminal flowering throughout their life cycles, whereas others produce both terminal and lateral flowers in either a synchronized or non-synchronized manner and thus form determinate or semi-determinate stems (Tian et al., 2010; Ping et al., 2014). At the center of this difference lies a regulatory process that determines whether, when, and where the vegetative shoot apical meristems (SAMs) transition into inflorescence meristems (IMs) and then into floral meristems (FMs) that form flowers (Bradley et al., 1997; Melzer et al., 2008; Liu et al., 2009; Wong et al.,

Published by the Molecular Plant Shanghai Editorial Office in association with Cell Press, an imprint of Elsevier Inc., on behalf of CSPB and IPPE, SIBS, CAS.

2009). Similar to flowering time (Cho et al., 2017), the plant stem growth habit associated with terminal flowering is a key adaptive trait regulated by both environmental signals and endogenous cues (Bradley et al., 1997; Tian et al., 2010; Ping et al., 2014; Liu et al., 2016). In soybean (*Glycine max*), stem growth habit is of particular importance as it affects plant height, flowering period, spatial distribution of flowers and pods, node production, maturity, water-use efficiency (WUE), environmental adaptability, and, ultimately, yield (Bernard, 1972; Specht et al., 2001; Heatherly and Elmore, 2004). Therefore, stem growth habit in soybean has been investigated for decades and remains one of the primary foci of current breeding programs worldwide.

Despite great variation of stem growth habit in soybean, most elite cultivars can be classified into three categories of stem architecture, commonly known as determinate, semi-determinate, and indeterminate types (Bernard, 1972). A determinate stem arises when apical stem growth abruptly ceases at the onset of floral induction, producing a thick stem because latitudinal growth (increasing stem girth) continues after apical growth (increasing stem length) has ceased. An indeterminate stem tip continues terminal growth as well as lateral growth, although both cease at the onset of seed filling, thus producing a stem that is tapered in thickness from base to tip. In the past decades, an increasing number of semi-determinate cultivars have been developed and deployed for soybean production. Semi-determinate cultivars produce stems with terminal racemes similar to those observed in determinate cultivars but show intermediate phenotypes for important agronomic traits such as plant height and node density.

An early study suggested that soybean stem growth habit was regulated by an epistatic interaction between two major loci, *Dt1* and *Dt2* (Bernard, 1972). The *Dt1* allele is completely or incompletely dominant over the *dt1* allele while the *Dt2* allele is completely dominant over the *dt2* allele (Bernard, 1972; Liu et al., 2007, 2010; Ping et al., 2014). In *Dt1Dt1* genetic backgrounds, *Dt2Dt2* genotypes produce semi-determinate stems whereas *dt2dt2* genotypes produce indeterminate stems. However, in *dt1dt1* genetic backgrounds the phenotype is determinate, demonstrating the epistatic interaction between the two loci at the phenotypic level. In our previous studies, we cloned both *Dt1* and *Dt2* (Tian et al., 2010; Ping et al., 2014) and elucidated their interaction at the molecular level (Liu et al., 2016). *Dt1* encodes a signaling protein in shoot meristems that prevents terminal flowering, and the transition from indeterminate to determinate stem growth habit was caused by independent human selection of four distinct single-nucleotide substitutions in the coding sequence during soybean domestication (Tian et al., 2010). *Dt2* encodes an MADS-domain transcription factor (TF) that directly binds to the promoter region of *Dt1* to repress its expression (Ping et al., 2014; Liu et al., 2016). Because the *Dt2* allele is mainly present in elite cultivars, it is deemed to be derived from a post-domestication gain-of-function mutation, which occurred within the gene's non-coding sequence, affecting its spatiotemporal expression (Ping et al., 2014).

Specific expression of *Dt2* was detected in the SAMs, rather than lateral meristems, of stem tips at the vegetative stage (Ping et al., 2014). However, differential expression of the *Dt2*/*dt2* locus was also observed in other tissues, such as leaves, between semi-determinate and indeterminate genotypes (Ping et al., 2014), raising the hypothesis that *Dt2* may play additional roles in modulating other morphological, physiological, and/or developmental traits. Stem growth habit is also implicated to be associated with leaf morphology and gas-exchange traits in soybean (Tanaka and Shiraiwa, 2009). A more recent study indicates that the semi-determinate growth habit adjusts the vegetative-to-reproductive balance and increases productivity and WUE in tomato (*Solanum lycopersicum*) (Vicente et al., 2015), although the genetic control of semi-determinacy differs between tomato and soybean (Elkind et al., 1991; Pnueli et al., 1998; Fridman et al., 2002; Ping et al., 2014).

To understand how the *Dt2* mutation modulates semi-determinacy and other traits of agronomic importance, we performed a comprehensive analysis that integrates chromatin immunoprecipitation sequencing (ChIP-seq), RNA sequencing (RNA-seq), profiling of microRNA (miRNA) expression and abundance of miRNAs, and phenotyping of *Dt2*/*dt2* isogenic lines and *Dt2* transgenic lines. This analysis not only identified divergent and convergent genetic pathways modulating multiple traits of agronomic importance, but also provides an understanding of how pleiotropy is systemically determined at the molecular level. From an application aspect, the findings from this work will facilitate optimization of plant architecture for enhanced yield potential and environmental resilience.

RESULTS

Genome-wide Identification of Dt2-Binding Sites: Distribution, *cis* Elements, and Target Genes

To dissect Dt2-mediated genetic pathways underlying stem growth habit and other pleiotropic traits, we identified *in vivo* Dt2-binding sites across the soybean genome by performing ChIP-seq using a highly specific Dt2 antibody (anti-Dt2), which was raised against a unique 19-amino-acid peptide in the K-box domain of the Dt2 protein (Liu et al., 2016). ChIP assays with anti-Dt2 and control antibodies (immunoglobulin G [IgG]) were performed using the stem tips collected from the semi-determinate soybean variety NE3001 at the vegetative 2 (V2) stage, when the first trifoliate leaflets were fully expanded but the second trifoliate leaflets were not yet unfolded. This is also the stage at which floral induction occurs in both apical and lateral meristems in semi-determinate soybeans (Ping et al., 2014; Liu et al., 2016). At this stage, *Dt2* is expressed at the highest level in stem tips, as detected by quantitative real-time PCR (qRT–PCR) (Ping et al., 2014). Consistent with the qRT–PCR data, high abundance of the Dt2 protein was detected in stem tips as well as leaves of NE3001 at the V2 stage by immunoblot analysis (Figure 1A). In addition, higher abundance of the Dt2 protein was detected in NE3001 and the semi-determinate *Dt2*-near-isogenic line (NIL) L62-364 with the Harosoy background than was detected in the indeterminate genotypes IA3023 and Harosoy (i.e., *dt2*-NIL) (Figure 1A), confirming our earlier deduction that *Dt2* and *dt2* differ in levels of expression (Ping et al., 2014; Liu et al., 2016).

Independent ChIP experiments from three biological replicates were conducted to identify DNA fragments bound by Dt2.

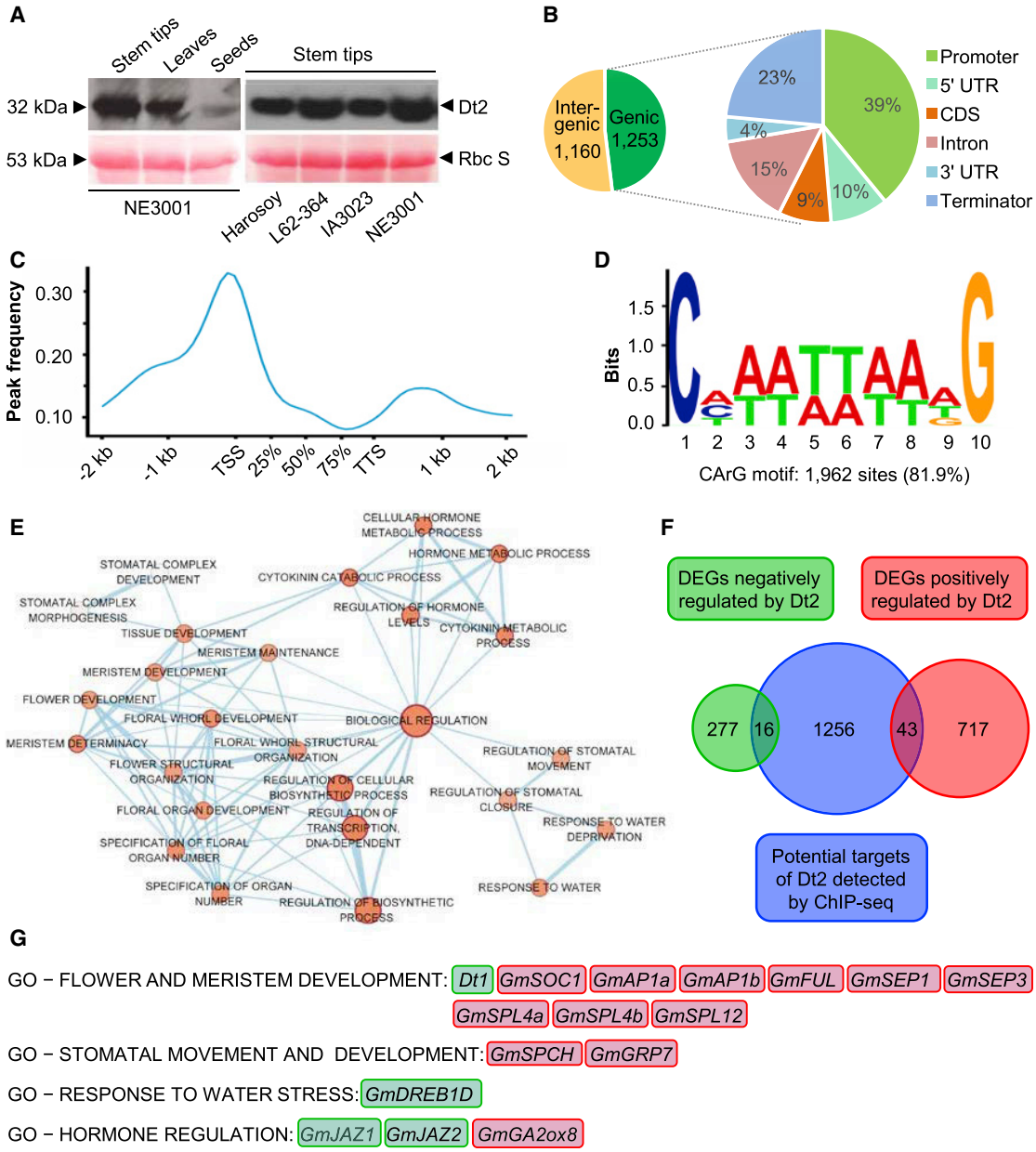

Figure 1. Genome-wide Identification of Dt2-Binding Sequences and Target Genes.

(A) Levels of Dt2 in total protein extracts were detected by western blot using the anti-Dt2 antibody. Ponceau S served as a loading control.

(B) Distribution of the locations of binding sites relative to target genes. Definitions: promoter is a sequence within 2 kb upstream of transcription start site; 3′ end is the sequence within 2 kb downstream of the transcription termination site; gene body includes 5′ UTR, CDS, intron, and 3′ UTR; intergenic is anything outside the above regions.

(C) The distribution of the CArG-box motif within the Dt2-binding regions.

(D) Motif analysis of Dt2-binding sequences using HOMER software. For the distribution of a single motif among the sequences, the parameter was set to zero or one per sequence.

(E) GO categories enriched in the Dt2 target genes were analyzed with BiNGO.

(F) Venn diagram showing a comparison between RNA-seq and ChIP-seq results. DEGs, differentially expressed genes.

(G) Gene ontology (GO) classification for DEGs with Dt2-binding sites detected.

See also Supplemental Figure 2.

Chromatin immunoprecipitation with qPCR (ChIP–qPCR) of the *Dt1* gene, which was previously confirmed to be directly bound by Dt2 (Liu et al., 2016), was used to evaluate the quality of the ChIP experiments. As shown in Supplemental Figure 1, a fragment harboring Dt2-binding sites in the promoter region of *Dt1* was highly enriched in DNA chromatin-immunoprecipitated (ChIPed) with anti-Dt2 in all three ChIP experiments. Thus, the sequences of all three ChIPed DNA samples were determined using the Illumina HiSeq 2500 platform. A total of ~282 million and ~182 million 100-bp single-end reads were obtained for Dt2

and IgG ChIPed samples, respectively, of which, ~226 million and ~173 million reads were uniquely mapped to the soybean reference genome (Schmutz et al., 2010; version 2.0, phytozome.org). Subsequently, a total of 2395 common peaks (Figure 1B and Supplemental Data 1), representing Dt2-binding sites across the entire genome, were detected in all three replicates by Model Based Analysis for ChIP-seq Data (MACS2 [Zhang et al., 2008]). Peaks only detected in one or two of the three replicates were excluded from further analyses.

Of the 2395 Dt2-binding sites detected by ChIP-seq, 1253 (52.32%) were located in genic regions, which comprise gene bodies and their flanking regulatory sequences, including 2-kb upstream regions that are assumed to harbor promoter regions and 2-kb downstream regions that are assumed to contain terminator regions, while the remaining sites were located in intergenic regions (Figure 1B and Supplemental Data 1). Of the 1253 sites in genic regions, 39.08%, 9.60%, 8.71%, 14.90%, 4.17%, and 23.58% were located in defined promoter regions, 5′ untranslated regions (5′ UTRs), coding sequences (CDS), introns, 3′ UTRs, and terminator regions, respectively (Figure 1B and Supplemental Data 1). The most frequent Dt2-binding sites in genic regions were located around transcription start sites (TSS) (Figure 1C). Given that the ChIP-seq peaks located in the defined terminator regions of putative Dt2 targets could be promoter regions of neighboring genes, the actual proportion of Dt2-binding sites located in promoter regions is most likely higher than that defined above.

According to the consensus sequences at the detected Dt2-binding sites, putative Dt2-binding motifs were predicted using the Hypergeometric Optimization of Motif EnRichment (HOMER) software (Heinz et al., 2010). Based on the predictions, the most abundant Dt2-binding motif is the CArG-box motif (Figure 1D), which was found in 81.9% of the Dt2-ChIP peaks. MADS-domain TFs are generally able to bind to the CArG box (Shore and Sharrocks, 1995; De Folter and Angenent, 2006). In addition, our previous study demonstrated that Dt2, an MADS-domain TF, directly binds to three CArG-box motifs in the promoter region of *Dt1* (Liu et al., 2016). These facts further bolster the authenticity of the Dt2-binding sites detected in this study. Additional motifs were detected in the Dt2-ChIP peaks (Supplemental Figure 2). These motifs may represent novel *cis* elements bound by Dt2 or could be *cis* elements bound by Dt2-interacting TFs. For example, the G-box motif, which is generally bound by basic helix-loop-helix (bHLH) and basic region leucine zipper TFs (Kawagoe and Murai, 1996), was detected in 30.3% of the Dt2-ChIP peaks.

In an attempt to deduce the possible functions of Dt2 in addition to its role as a direct repressor of *Dt1*, 1315 putative target genes of Dt2 were functionally annotated by gene ontology (GO) analysis. For GO analysis, we particularly focused on target genes most significantly related to "biological regulation." As shown in Figure 1E, some putative Dt2 targets, as expected, were predicted to be associated with meristem development, maintenance, and determinacy, as well as flower development and hormone metabolic processes. Interestingly, some putative Dt2 targets were predicted to be associated with stomatal development and morphogenesis, with regulation of stomatal movement and closure, and with responses to water deprivation (Figure 1E and 1G). These genes were further annotated by performing BLAST searches against nucleotide and protein databases, particularly those of *Arabidopsis*, at GenBank (Supplemental Data 2 and Supplemental Table 1).

Extensive Expression Changes of Genes Modulating Biological Processes Triggered by *Dt2*

To establish the regulatory roles of Dt2, we identified the Dt2 targets and additional genes whose transcriptional activities are associated with relative abundance of the *Dt2*/*dt2* transcripts based on RNA-seq analysis. Transcriptomic data from the V2-stage stem tips of an indeterminate (*dt2*) soybean variety (Thorne) and a *Dt2*-overexpression transgenic line (917-65) of Thorne (Ping et al., 2014) were generated and compared, and a total of 1053 differentially expressed genes (DEGs) between Thorne and the *Dt2* transgenic line were detected (Figure 1F and Supplemental Data 1). These include 293 genes downregulated and 760 genes upregulated by *Dt2*overexpression. Some of the DEGs were predicted to be associated with developmental maturation, immune system process, and cell differentiation (Supplemental Figure 3). Of these downregulated and upregulated genes, 16 and 43 are putative Dt2 targets, respectively (Figure 1F). Among these 59 DEGs targeted by Dt2 and those previously detected by qRT–PCR (Ping et al., 2014; Liu et al., 2016), 10 are associated with flower development and/or meristem development, two are associated with hormone regulation, one is associated with response to drought stress, and two are associated with stomatal development/opening, according to GO analysis and homology-based functional annotation (Figure 1G). The 994 DEGs that are not Dt2 targets, based on the ChIP-seq analysis, were considered to be genes indirectly regulated by *Dt2* and were excluded from further analyses.

Dual Roles of *Dt2* in Modulating Semi-determinacy: Activator and Repressor

We further validated the 10 differentially expressed *Dt2* targets that were annotated to be associated with "meristem and/or flower development" (Figure 1G). These include *Glyma.01G194300*—the functional ortholog of *Arabidopsis TFL1* (*Dt1*), *Glyma18G224500*—the functional ortholog of *Arabidopsis* floral integrator gene *SOC1* (*GmSOC1*), *Glyma01G06200* and *Glyma.02G121600*—two orthologs of *Arabidopsis* floral identity gene *AP1* (*GmAP1a* and *GmAP1b*), *Glyma.05G018800*—an ortholog of *Arabidopsis* floral identity gene *FUL* (*GmFUL*), *Glyma.20G153700*—a closely related homolog of *Arabidopsis SEP3* (*GmSEP3*), and *Glyma.13G255200*—a closely related homolog of *Arabidopsis AGL21* (*GmAGL21*). Dt1 is a repressor of flowering encoding a phosphatidylethanolamine-binding protein (Simon et al., 1996). *SQUAMOSA PROMOTER-BINDING PROTEIN-LIKE* genes (*SPLs*) have a highly conserved SBP (SQUAMOSA PROMOTER-BINDING PROTEIN) domain that plays vital roles in plant growth and development (Schmid et al., 2003). *SOC1*, *AP1*, *FUL*, *SEP3*, and *AGL21* in *Arabidopsis* all encode MADS-domain TFs and are activators of lateral flowering (Liu et al., 2009; Yant et al., 2009; Fornara et al., 2010; Smaczniak et al., 2012). If the soybean orthologs of these *Arabidopsis* genes are also activators of lateral flowering in soybean, the activation of these genes by spatiotemporal

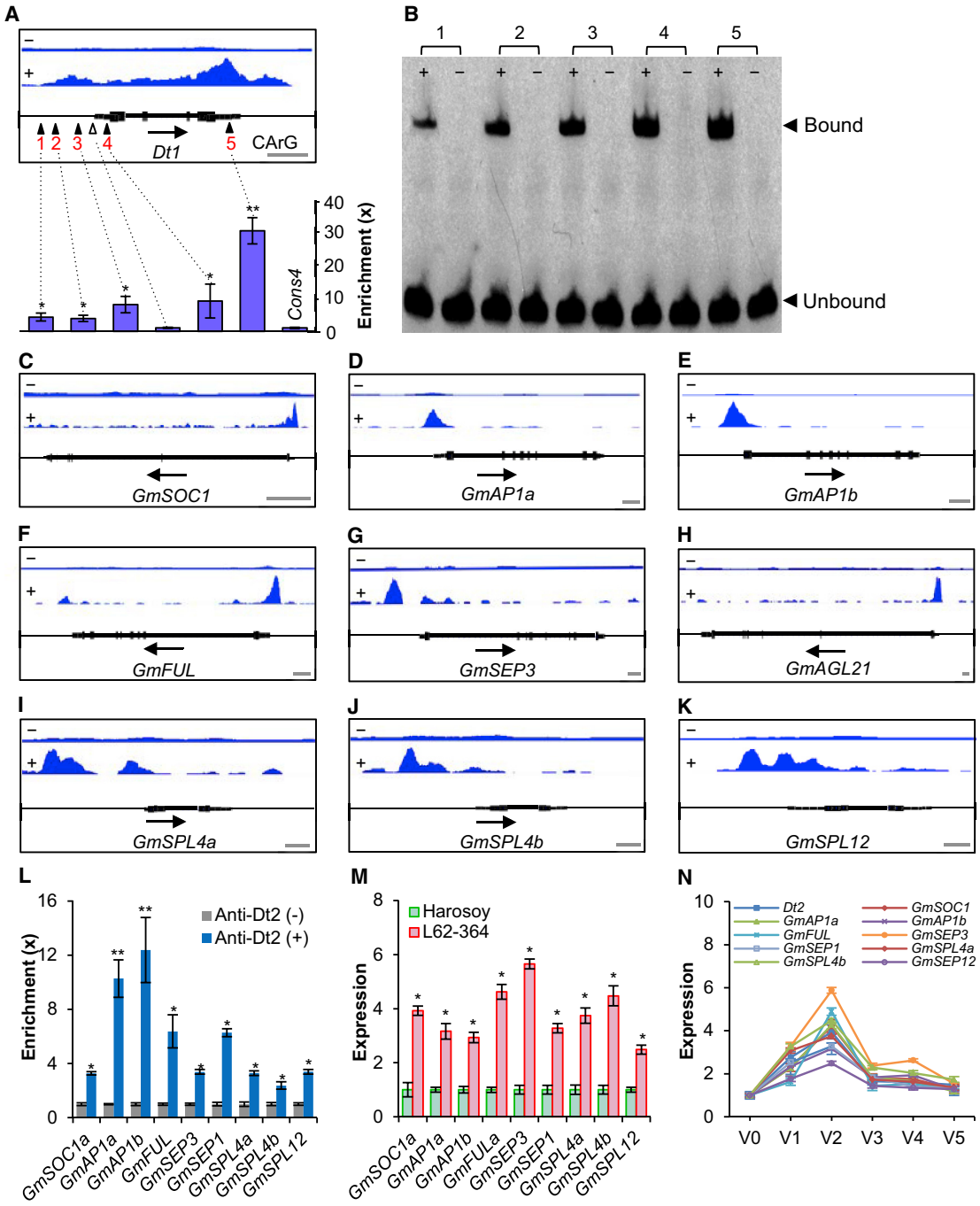

Figure 2. Validation and Expression Analyses of Selected Dt2 Target Genes.

(A) Relative enrichment of Dt2-binding fragments from the regulatory region of *Dt1* detected by ChIP–qPCR, using a fragment from *Cons4* as a control. Upper panel: gene structures are shown in black. Peak heights for both positive (+) and negative control (−) are shown on the same scale, relative to the maximum number of sequence reads. Gray scale bar represents 500 bp. Lower panel: physical locations of the five fragments each harboring a putative CArG box (solid triangles) and a randomly chosen fragment without a putative CArG box (a triangular frame) are shown in the schematic diagram. The relative enrichment of the *Cons4* fragment was set as 1.0 and those of other fragments were adjusted accordingly. Values are shown as mean ± standard errors of the mean (SEM) from three biological replicates. Student's *t*-test, $^{*}P < 0.05$; $^{**}P < 0.01$.

(B) Dt2-binding sites in the regulatory region of *Dt1* validated by EMSA. Samples 1 to 5 represent fragments in the *Dt1* promoter region containing the five CArG motifs as shown in **(A)**. The "+" and "−" indicate reactions with and without unlabeled competitor probes, respectively. Upper and lower arrowheads indicate probes bound and unbound by the Dt2-6×His fusion protein, respectively.

(C–K) The indicated target gene structures are shown in black. Black arrowheads indicate the direction of transcription. Peak heights for both positive (+) and negative controls (–) are shown on the same scale, relative to the maximum number of sequence reads. Gray scale bars represent 500 bp.

(legend continued on next page)

expression of *Dt2* in SAMs would be essential for initiating apical terminal flowering as well.

We previously identified three Dt2-binding CArG motifs in the promoter region of *Dt1* and further confirmed that all three motifs are essential for sufficient repression of *Dt1* transcription by Dt2 to implement semi-determinate stem growth (Liu et al., 2016). In this study, ChIP-seq detected a new Dt2-binding motif, which is located in the 3′ UTR of *Dt1* (Figure 2A). This newly identified Dt2-binding site as well as four previously identified binding sites were validated by both ChIP–qPCR and an electrophoretic mobility shift assay (EMSA) (Figure 2A and 2B). Strikingly, the ChIPed fragments harboring this newly identified Dt2-binding site showed an extremely high level of enrichment, which was even higher than that of the ChIPed fragments from all four Dt2-binding sites in the promoter region of *Dt1*, indicating the significance of the 3′ UTR CArG motif for implementation of Dt2 function.

Our previous work revealed spatiotemporal co-expression of *Dt2* and *GmSOC1* in SAMs within stem tips of NE3001, where GmSOC1 interacts with Dt2, and also directly binds to the *Dt1* regulatory sequence to fulfill the repression of *Dt1* transcription (Liu et al., 2016). However, the specific TF(s) inducing *GmSOC1* expression in the SAM were unknown. The ChIP-seq data in this study revealed a Dt2-binding peak harboring a CArG motif in the promoter region of *GmSOC1*. The binding of Dt2 to this motif was validated by ChIP–qPCR (Figure 2C). This suggests that Dt2 is most likely the direct inducer of *GmSOC1* expression in the SAM. Dt2-binding peaks harboring CArG motifs were also identified in the promoter regions of *GmAP1a*, *GmAP1b*, *GmFUL*, *GmSEP3*, *GmAGL21*, *GmSPL4a*, *GmSPL4b*, and *GmSPL12*, and binding of Dt2 to some of the CArG motifs in these genes was validated by ChIP–qPCR (Figure 2D–2L). Similar to *GmSOC1*, *GmAP1a*, *GmAP1b*, *GmFUL*, *GmSEP3*, *GmAGL21*, *GmSPL4a*, *GmSPL4b*, and *GmSPL12* were all expressed at significantly higher levels in stem tips at the V2 stage in the *Dt2*-NIL L62-364 than in the *dt2*-NIL Harosoy (Figure 2M), suggesting that these TFs in soybean are activators of terminal flowering. Moreover, all of these MADS-domain factor genes exhibited co-expression in stem tips of NE3001 from the developmental stages V0 (when the unifoliate leaves start to unroll) to V5 (when the fifth trifoliate leaves have developed) (Figure 2N). Hence, although Dt2 was identified to be the key gene that interacts with *Dt1* to promote terminal flowering, the formation of semi-determinacy is indeed a considerably dynamic process that involves: (1) activation of a set of MADS-domain TF genes including *GmSOC1*, *GmAP1a*, *GmAP1b*, *GmFUL*, *GmSEP3*, and *GmAGL21* by spatiotemporal expression of Dt2 in SAMs; (2) development of a TF complex likely consisting of homodimers, heterodimers, and tetramers that binds the promoter and 3′ UTR regions of *Dt1* and fulfills repression of its transcription; and (3) transition of vegetative SAMs to IMs and then FMs that form terminal flowers.

Dt2-Mediated Genetic Pathways Responsive to Drought Stress

Of the 59 detected Dt2 targets that showed differential expression between Thorne and the *Dt2*-overexpression line, *Glyma09G147200* was predicted to be associated with "response to drought stress" (Figure 1G and Supplemental Table 1). This gene is most closely related to *AT5G51990*, which encodes the dehydration-responsive element-binding protein 1D (*DREB1D*) in *Arabidopsis*, and thus is designated as *GmDREB1D*. A Dt2-binding peak was detected in the promoter region of *GmDREB1D*, which carries five putative Dt2-binding CArG motifs, two of which (third and fourth) were validated by ChIP–qPCR (Figure 3A). The binding of Dt2 to a fragment harboring the fourth motif was further confirmed by an EMSA (Supplemental Figure 4). In addition, a transcriptional regulation activity assay in protoplasts revealed that Dt2 repressed the expression of the *GmDREB1D* promoter driving the expression of the luciferase (LUC) reporter gene (Figure 3B). These observations indicate that Dt2 is a direct repressor of *GmDREB1D*. To understand the nature of Dt2–*GmDREB1D* interaction, we analyzed expression patterns of *GmDREB1D* in four *Dt2*- and *Dt1*-NILs. These NILs are Harosoy (*dt2*/*dt2*;*Dt1*/*Dt1*, indeterminate), L62-364 (*Dt2*/*Dt2*;*Dt1*/*Dt1*, semi-determinate), L62-973 (*dt2*/*dt2*;*dt1*/*dt1*, determinate), and L67-3256 (*Dt2*/*Dt2*;*dt1*/*dt1*, determinate) (Figure 3C). Consistent with the expression patterns observed in the *Dt2*-overexpression lines and the control, *GmDREB1D* had a significantly lower level of expression in V2-stage stem tips of the *Dt2*-NILs L62-364 and L67-3256 than in the *dt2*-NILs Harosoy and L62-973, respectively (Figure 3D). The expression levels of *GmDREB1D* exhibited a negative association with those of *Dt2* in step tips of L62-364 from developmental stages V0 to V5 (Figure 3E). However, there was not a significant decrease in *GmDREB1D* expression levels in V2-stage stem tips either between Harosoy and L62-973 or between L62-364 and L67-3256 (Figure 3D), suggesting that the Dt2–*GmDREB1D* interaction is independent of the *Dt1*/*dt1* locus.

DREB1D is expressed at higher levels in response to water deprivation in *Arabidopsis* (Lata and Prasad, 2011). A recent study demonstrated that overexpression of *Arabidopsis DREB1D* in soybean enhances drought tolerance (Guttikonda et al., 2014). Thus, we hypothesized that repression of *GmDREB1D* by Dt2 may result in reduced drought tolerance. To test this hypothesis, we compared responses to drought stress in the variety Thorne and three *Dt2*-overexpression lines (917-55, 917-56, and 917-65) in the Thorne background (*dt2*/*dt2*;*Dt1*/*Dt1*) (Figure 3F). Two

(L) ChIP–qPCR validation for selected Dt2 target genes related to flowering and flower development. ChIP–qPCR was used to verify potential Dt2-binding sites using a Dt2-antibody-treated sample and a sample with no Dt2-antibody treatment as a control. The relative enrichment of the fragments in the no Dt2-antibody treatment sample was set as 1.0 and those of other fragments were adjusted accordingly. Values are shown as mean ± SEM from three biological replicates. Asterisks indicate a significant change (*$P < 0.05$; **$P < 0.01$; Student's *t*-test).

(M) Expression of target genes in stem tips of different genotypes detected by qRT–PCR. Expression levels are relative to expression of *Cons4* and shown as mean ± SEM from three biological replicates. Asterisks indicate a significant change (*$P < 0.05$; Student's *t*-test).

(N) Expression patterns of *Dt2* and Dt2 target genes. Expression levels of flowering- and flower development-related genes in stem tips of L62-364 from the V0 to V5 stages. Values are shown as mean ± SEM from three biological replicates. Expression level of each gene/allele at the V0 stage, when the unifoliate leaves unroll, was set as 1, and those at other stages were adjusted accordingly.

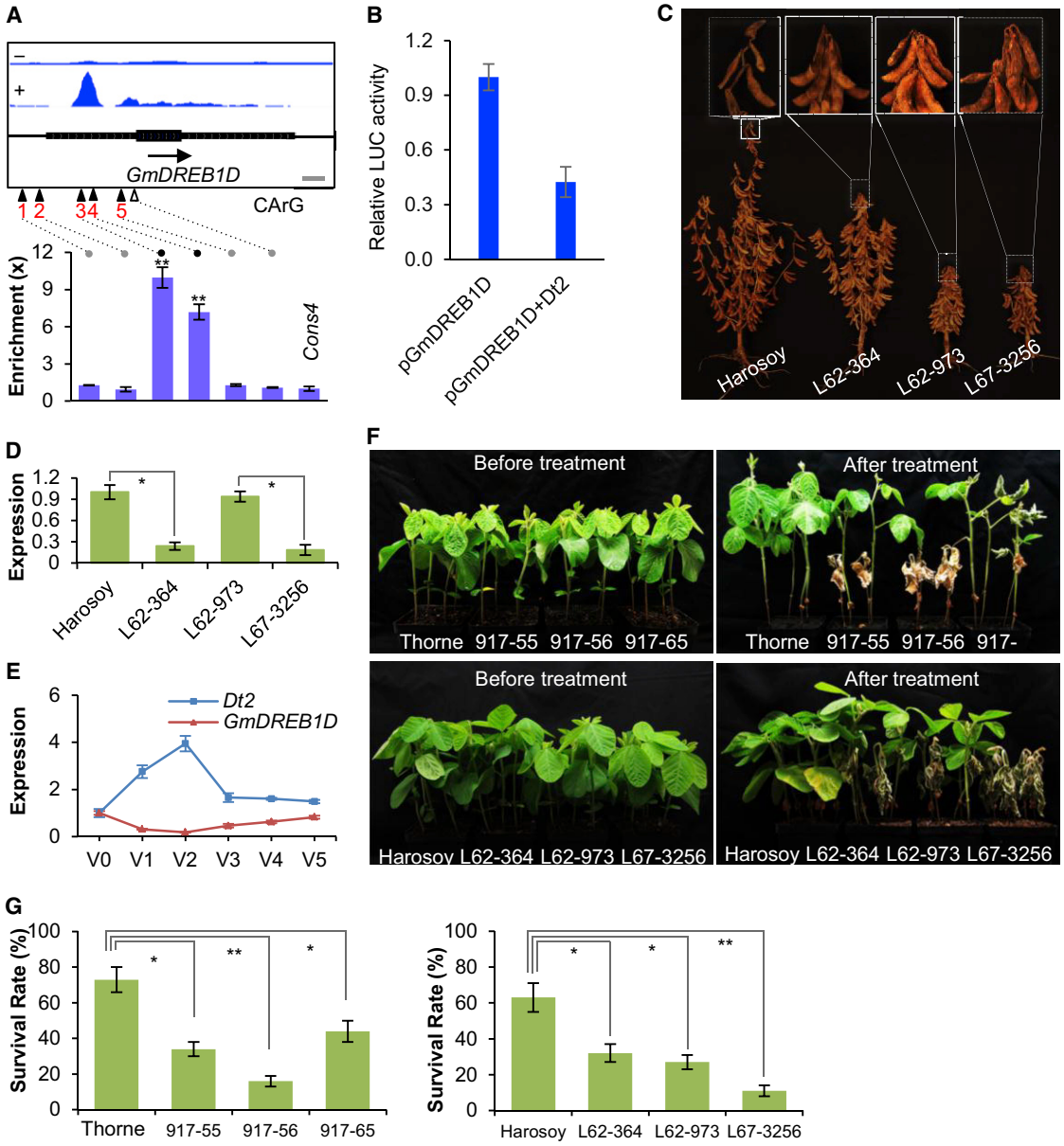

Figure 3. *Dt2* Appears to Be Responsive to Drought Stress.

(A) Relative enrichment of fragments from the regulatory region of *GmDREB1D* by anti-Dt2 detected by ChIP–qPCR, using a fragment from *Cons4* as a control. Physical locations of the putative CArG boxes (solid triangles, numbered in order) and a fragment without a CArG box (hollow triangle) are shown. The relative enrichment of the *Cons4* fragment was set as 1.0 and those of other fragments were adjusted accordingly. Values are shown as mean ± SEM from three biological replicates.

(B) Transient transcriptional assay of *GmDREB1D* regulated by Dt2 in soybean protoplasts. pGmDREB1D represents the promoter of the *GmDREB1D* gene. Values are shown as mean ± SD from three independent experimental replicates. LUC, luciferase.

(C) *Dt2*-NILs lines with a distinct stem growth habit. From right to left: indeterminate line Harosoy (*dt2*/*dt2*;*Dt1*/*Dt1*), semi-determinate line L62-364 (*Dt2*/*Dt2*;*Dt1*/*Dt1*), determinate line L62-973 (*dt2*/*dt2*;*dt1*/*dt1*), and determinate line L67-3256 (*Dt2*/*Dt2*;*dt1*/*dt1*).

(D) Expression of *GmDREB1D* in stem tips of different genotypes detected by qRT–PCR. Expression levels are relative to expression of *Cons4* and shown as mean ± SEM from three biological replicates. Asterisks indicate a significant change (*$P < 0.05$; Student's *t*-test).

(E) Expression levels of *GmDREB1D* in stem tips of L62-364 from the V0 to V5 stages. Values are shown as mean ± SEM from three biological replicates. Expression level of each gene/allele at the V0 stage was set as 1, and those at other stages were adjusted accordingly.

(F) The phenotype of seedlings of the Dt2 transgenic lines and *Dt2*-NILs before and after drought and recovery treatment (drought for 5 days and recovery for 7 days).

(G) Survival rate of the Dt2 transgenic lines and *Dt2*-NILs after drought and recovery treatment. Data are mean ± SD (>15 plants per line) from three biological replicates. Student' s *t*-test: *$P < 0.05$, **$P < 0.01$.

See also Supplemental Figure 3.

sets of the four lines were planted in the greenhouse, with one set watered regularly to the V1 stage followed by drought stress for 5 days, and the other (control) set was watered regularly until the plants were phenotyped. Three replicates of the experiments were performed. This experimental design allowed the plants to be drought-stressed around the V2 stage, when *Dt2* was expressed at the highest level and *GmDREB1D* was expressed at the lowest level (Figure 3E). As exemplified in Figure 3F, the *Dt2*-overexpression lines were more sensitive to drought stress than the control, based on visual observations as well as survival rates of plants of drought-stressed lines upon water recovery in all three replicates (Figure 3G). These observations, together with the previous finding that ectopic expression of *Arabidopsis DREB1D* enhances drought tolerance in soybean (Guttikonda et al., 2014), suggest that the reduced expression of *GmDREB1D* mediated by Dt2 is, at least partially, responsible for reduced tolerance to drought stress in the semi-determinate *Dt2*-overexpression lines compared with the indeterminate control.

Nevertheless, the effects of ectopic expression of *Dt2* in the transgenic lines may not accurately reflect the effects of spatio-temporal expression of *Dt2* and *GmDREB1D* on the plant's response to drought stress. In addition, semi-determinate plants and indeterminate plants often have different flowering times (Kuroda et al., 1998), which are often linked with tolerance to abiotic stress (Tanaka and Shiraiwa, 2009). Thus, it was unclear whether the sensitivity of semi-determinate plants to drought stress is partially a pleiotropic effect of the Dt2–*Dt1* interaction, in addition to the Dt2–*GmDREB1D* interaction. To address this question, we assessed the drought stress responses of four *Dt2*- and *Dt1*-NILs with the NIL background genotype Harosoy, following a similar experimental design as described above. As shown in Figure 3G, the survival rate of Harosoy was significantly higher than that of all other NILs, indicating that the *dt1* mutation was indeed responsible for reduction of tolerance to drought stress. In addition, the survival rate of L67-3256 was significantly lower than that of L62-973, indicating the involvement of an additional Dt2-mediated pathway(s), rather than the Dt2–*Dt1* pathway, in response to drought stress.

Dt2 Directly Regulates Putative Genes Associated with Stomatal Development and Activity

We further analyzed the two putative Dt2 targets (*Glyma.13G040100* and *Glyma.11G117400*) that were predicted to be associated with "stomatal development/movement" (Figure 1G and Supplemental Table 1). *Glyma.13G040100* is an ortholog of *Arabidopsis SPEECHLESS* (*SPCH*), which encodes a bHLH TF (Macalister et al., 2007), and is designated as *GmSPCH*. *Glyma.11G117400* is closely related to an *Arabidopsis* gene encoding *glycine-rich RNA-binding protein 7* (*GRP7*) (Kim et al., 2008). The Dt2-binding peak detected in the promoter region and flanking sequences of *GmSPCH* contains four putative Dt2-binding CArG motifs. As shown in Figure 4A, fragments containing the third and fourth putative CArG boxes were enriched by greater than 4- to 6-fold compared with the control DNA fragments amplified from the soybean ATP-binding cassette transporter gene *Cons4* in the same genome, suggesting that Dt2 is a direct regulator of *GmSPCH*, whereas the first and fourth putative CArG boxes were not enriched compared with the control.

The binding of Dt2 to a fragment containing the fourth CArG motif was further confirmed by EMSA (Supplemental Figure 4). The Dt2-binding peak detected in the promoter region and flanking sequences of *GmGRP7* harbors three putative Dt2-binding CArG motifs. As shown in Figure 4B, a fragment containing the third putative CArG box was enriched by greater than 6-fold compared with the controls. The binding of Dt2 to this fragment was further confirmed by EMSA (Supplemental Figure 4). In addition, the specific binding and activation of *GmSPCH* and *GmGRP7* by Dt2 were further validated using a transient expression system (Figure 4C). These observations indicate that Dt2 is a direct activator of both genes.

Consistent with what we observed in the *Dt2*-overexpression lines and the control, both *GmSPCH* and *GmGRP7* showed significantly higher levels of expression in V2-stage stem tips of the *Dt2*-NILs L62-364 and L67-3256 than in those of the *dt2*-NILs Harosoy and L63-973 (Figure 4D). Both *GmSPCH* and *GmGRP7* were co-expressed with *Dt2* in stem tips of L62-364 from developmental stages V0 to V5 (Figure 4E). *GmSPCH* and *GmGRP7* also exhibited overall higher levels of expression in leaves of the *Dt2*-NIL L62-364 than in those of the *dt2*-NIL Harosoy, particularly at the V2 stage (Figure 4F and 4G), suggesting that the *Dt2* and *dt2* alleles may differentially regulate the expression of their targets in leaves of semi-determinate and indeterminate plants, and that V2 may also be the key stage at which *Dt2* regulates the expression of its targets in leaves.

In *Arabidopsis*, *SPCH* is necessary for asymmetric cell divisions that establish the stomatal lineage (Macalister et al., 2007), and a mutation at the *SPCH* locus results in stomataless leaves or severe reductions in the number of stomata in the leaves (Marcos et al., 2017). However, because differential expression of *GmSPCH* between the *Dt2*- and *dt2*-NILs mainly occurs in developing stem tips and trifoliate leaves around the V2 stage (Ping et al., 2014; Figure 4F), when the trifoliate leaves are far from full expansion, whether the *Dt2* and *dt2* alleles differentially affect the dynamic stomatal developmental process could not be determined at this stage. However, because different responses of the *Dt2* and *dt2* genotypes to drought stress were detected around the V2 stage, we anticipate that differential effects of the *Dt2* and *dt2* alleles, if any, on the regulation of stomatal development (e.g., stomatal density and patterning) at such an early and short developmental stage is likely minimal.

The *Arabidopsis GRP7* affects plant growth and stress tolerance under high salt and dehydration stress conditions, and also confers freezing tolerance, particularly via the regulation of stomatal opening and closing by guard cells (Kim et al., 2008). Although it is unknown whether *GmGRP7* possesses a *GRP7*-like function modulating stomatal aperture in soybean under drought stress, the expression level of *GmGRP7* in L62-364 was significantly higher than that in Harosoy, and the expression level of *GmGRP7* in L67-3256 was significantly higher than that in L62-973 (Figure 4D). By contrast, no significant difference of *GmGRP7* in expression level was observed between Harosoy and L62-973 or between L62-364 and L67-3256 (Figure 4D), suggesting that the Dt2–*Dt1* pathway is not involved in modulation of the trait(s) affected by the Dt2–*GmGRP7* pathway. If *GmGRP7* in soybean indeed functions as *GRP7* does in *Arabidopsis*, the reduced tolerance of semi-determinate plants to drought stress relative

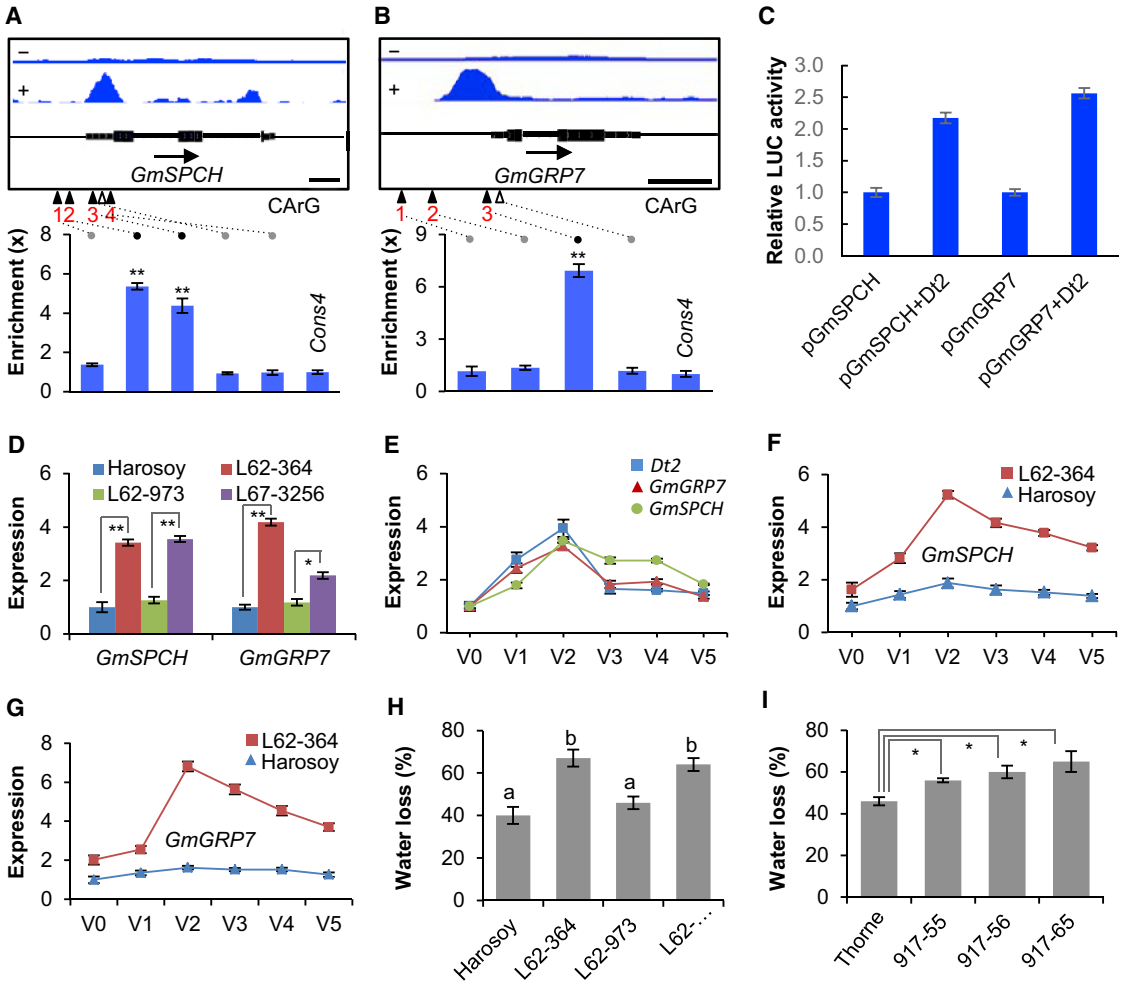

Figure 4. Dt2 Directly Regulates Target Genes *GmSPCH* and *GmGRP7*, which Appear to Modulate Stomatal Development and Opening.

(A and B) Relative enrichment of fragments from the regulatory region of *GmSPCH* **(A)** and *GmGRP7* **(B)** by anti-Dt2 detected by ChIP–PCR, using a fragment from *Cons4* as a control. Physical locations of the putative CArG boxes are indicated by solid triangles and numbered in order. The relative enrichment of the *Cons4* fragment was set as 1.0 and those of other fragments were adjusted accordingly. Values are shown as mean ± SEM from three biological replicates.

(C) Transient transcriptional assays of *GmSPCH* and *GmGRP7* regulated by Dt2 in soybean protoplasts. pGmSPCH and pGmGRP7 represent the promoters of the respective genes. Values are shown as mean ± SD from three independent experimental replicates. LUC, luciferase.

(D) Expression of *GmSPCH* and *GmGRP7* in stem tips of different genotypes detected by qRT–PCR. Expression levels are relative to expression of *Cons4* and shown as mean ± SEM from three biological replicates. Asterisks indicate a significant change (*$P < 0.05$, **$P < 0.01$; Student's *t*-test).

(E) Expression levels of *GmSPCH* and *GmGRP7* in stem tips of L62-364 from the V0 to V5 stages. Values are shown as mean ± SEM from three biological replicates. Expression level of each gene at the V0 stage was set as 1, and those at other stages were adjusted accordingly.

(F and G) Expression levels of *GmSPCH* **(F)** and *GmGRP7* **(G)** in leaves of L62-364 and Harosoy from the V0 to V5 stages. Values are shown as mean ± SEM from three biological replicates. Expression level of each gene in Harosoy at the V0 stage was set as 1, and those of other samples were adjusted accordingly.

(H and I) Water loss detected in indicated plants grown to the V2 stage under a 10-h diurnal photoperiod. Values are shown as mean ± SEM (four plants per line) from seven biological replicates. Different letters a and b indicate significant differences between lines. *$P < 0.05$; Student's *t* test.

to indeterminate plants, as detected in this study, would be explained by the enhancement of *GmGRP7* expression by *Dt2*. The gene expression pattern described above is consistent with the rates of water loss observed in the four NILs (Figure 4H): the percentages of water loss in L62-364 and L67-3256 were significantly higher than those in Harosoy and L62-973, respectively. If the rate of water loss is most likely modulated by the Dt2–*GmGRP7* pathway, it appears to be independent of the *Dt1*/*dt1* locus as well. Higher percentages of water loss were also observed in the Dt2-transgenic lines compared with the indeterminate control (Figure 4I), further suggesting that the *Dt2* mutation is indeed the trigger for the high rates of water loss, which are likely associated with WUE.

To further understand the functional roles of the detected genetic pathways in modulating plant response to drought stress, we analyzed the expression patterns of *GmDREB1D*, *GmSPCH*, *GmGRP7*, and *Dt2*/*dt2* in the V2-stage leaves of Harosoy and

the *Dt2*-NIL L62-364 in response to drought stress. As shown in Supplemental Figure 5, all four genes responded to the stress at the transcriptional level; nevertheless, the degree of change in *GmDREB1D*, *GmSPCH*, and *GmGRP7* expression in response to the stress in L62-364 was much greater than that in Harosoy. These observations suggest that *Dt2* is directly responsible for the reduced drought tolerance of semi-determinate plants through direct regulation of these targets involved in drought stress response (Supplemental Figure 5).

Dt2 Directly Regulates Putative Genes Associated with Hormone Signaling

Of the 59 detected Dt2 targets that showed differential expression between Thorne and the *Dt2*-overexpression line, *Glyma.11G038600* and *Glyma.01G204400* are closely related to the *Arabidopsis* genes encoding jasmonate-zim-domain protein 1 (JAZ1) and jasmonate-zim-domain protein 2 (JAZ2), and were dubbed *GmJAZ1* and *GmJAZ2*, respectively. It was suggested that, under stress conditions, plant hormone the jasmonic acid (JA) induces the degradation of JAZ proteins involved in transcriptional repression of the *flowering locus T* (*FT*) to promote flowering in *Arabidopsis* (Zhai et al., 2015). As both *GmJAZ1* and *GmJAZ2* are downregulated by Dt2, the effect of Dt2 on flowering time may be partially associated with JA signaling, particularly under the drought condition. In addition, *Arabidopsis jaz2* mutants were found to be partially impaired in pathogen-induced stomatal closing (Gimenez-Ibanez et al., 2017); thus, downregulation of *GmJAZ2* by Dt2 may affect stomatal closure in semi-determinate soybean plants. A third differentially expressed Dt2 target that is putatively associated with hormone signaling is *Glyma.05G063300*, which is a close homolog of the *Arabidopsis* gene encoding gibberellin 2-β-dioxygenase 8 (GA2ox8), and was dubbed *GmGA2ox8*. Previous work has demonstrated that increased expression of *GA2ox8* results in decreased levels of active gibberellins (GAs) and corresponding dwarf phenotypes in *Arabidopsis* and tobacco (Schomburg et al., 2003). As *GmGA2ox8* was upregulated by *Dt2*, the reduced plant height of semi-determinate plants relative to indeterminate plants may be partially caused by increased expression of *GmGA2ox8*, which is associated with GA signaling. In addition to these three Dt2 targets, a number of DEGs between Thorne and the Dt2 transgenic overexpression line were homologs/orthologs of *Arabidopsis* genes involved in various pathways responsive to GA, JA, cytokinin, auxin, and ethylene that regulate plant growth and development (Supplemental Data 2).

Dt2 Directly Regulates miRNA Genes that Produce miRNAs Associated with Development and Stress Responses

miRNAs have been identified as key players regulating plant growth, development, and stress responses (Kidner and Martienssen, 2005; Teotia and Tang, 2015). To understand whether and/or how the Dt2 mutation may trigger miRNA-mediated regulatory pathways underlying these pleiotropic traits, we identified miRNA precursor genes that are directly targeted and regulated by Dt2. A total of 22 putative Dt2-binding miRNAs were identified by ChIP-seq (Supplemental Data 3). The binding of Dt2 to CArG motifs in the putative promoter regions of these miRNAs was validated by ChIP–qPCR (Supplemental Figure 6A). The relative abundances of the miRNAs produced by these miRNA genes in stem tips of the *Dt2*-NIL L62-364 and *dt2*-NIL Harsoy were measured following a protocol described earlier (Zhao et al., 2015). As shown in Supplemental Figure 6B, the abundances of 17 miRNAs in the *Dt2*-NIL were significantly higher than those in the *dt2*-NIL, while the abundances of five miRNAs in the *Dt2*-NIL were significantly lower than those in the *dt2*-NIL, indicating that Dt2 functions as either an activator or repressor of these miRNAs. The potential regulatory roles of these miRNAs were annotated based on their miRNA counterparts in *Arabidopsis* (Supplemental Data 3). The predicted targets of these miRNAs are listed in Supplemental Data 4.

Two families of miRNAs, miR156 and miR172, have been identified as key miRNAs regulating flowering time in multiple plants (Spanudakis and Jackson, 2014; Teotia and Tang, 2015). In *Arabidopsis*, miR156 targets a few genes encoding SPL TFs to repress the juvenile-to-adult phase transition and flowering (Xu et al., 2016), whereas miR172 targets a gene encoding floral homeotic protein APETALA 2 (AP2) to promote the juvenile-to-adult phase transition and flowering (Aukerman and Sakai, 2003). A recent study in rice demonstrates that knockdown of miR166 increases the expression of *HOMEODOMAIN-CONTAINING PROTEIN 4* (*OsHB4*), a member of the HD-Zip III family, resulting in reduced stomatal conductance, decreased transpiration rate, and enhanced drought resistance (Zhang et al., 2018). Based on these observations, we hypothesized that different physiological traits (such as stomatal conductance) and responses to drought stress between the *Dt2*- and *dt2*-NILs are partially due to different abundances of miR156h, miR172c, and miR166n, which are bound by the Dt2 protein.

To address our hypothesis, we first examined the expression levels of the predicted target genes of miR156h, miR172c, and miR166n in the V2-stage stem tips of the *Dt2*-NIL L62-364 and the *dt2*-NIL Harosoy, then identified predicted target genes of these miRNAs that are differentially expressed between the two NILs, and finally determined whether a DEG is truly a target of an miRNA using 5′ rapid amplification of cDNA ends (5′ RACE), which was followed by sequencing of the amplified fragments. Only the predicted miR156h, miR172c, and miR166n targets in soybean that are closely related to *Arabidopsis SPL* genes targeted by miR156, the *Arabidopsis AP2* gene targeted by miR172, or the rice *OsHB4* gene targeted by miR166, were included in these analyses. There are 10 predicted miR156h targets closely related to *Arabidopsis SPL* genes (Supplemental Data 4), of which *GmSPL2a*, *GmSPL6a*, and *GmSPL9a* showed significantly higher levels of expression in the V2-stage stem tip of the *Dt2*-NIL L62-364 than in that of the *dt2*-NIL Harosoy (Figure 5A), and the cleavage sites of miR156h within the transcripts of these three genes were confirmed by 5′ RACE (Figure 5D and Supplemental Table 2). Four orthologs of *Arabidopsis AP2* were predicted to be miR172c targets, of which *GmAP2a* and *GmAP2b* showed significantly lower levels of expression in the V2-stage stem tip of the *Dt2*-NIL than in that of the *dt2*-NIL (Figure 5C), and the cleavage sites of miR172c within the transcripts of these two genes were confirmed by 5′ RACE (Figure 5D and Supplemental Table 2). Only two predicted miR166n targets (*GmHB4a* and *GmHB4b*) are closely related to *Arabidopsis HB15*, which corresponds to rice *OsHB4*, and only *GmHB4a* was targeted by miR166n (Figure 5D and

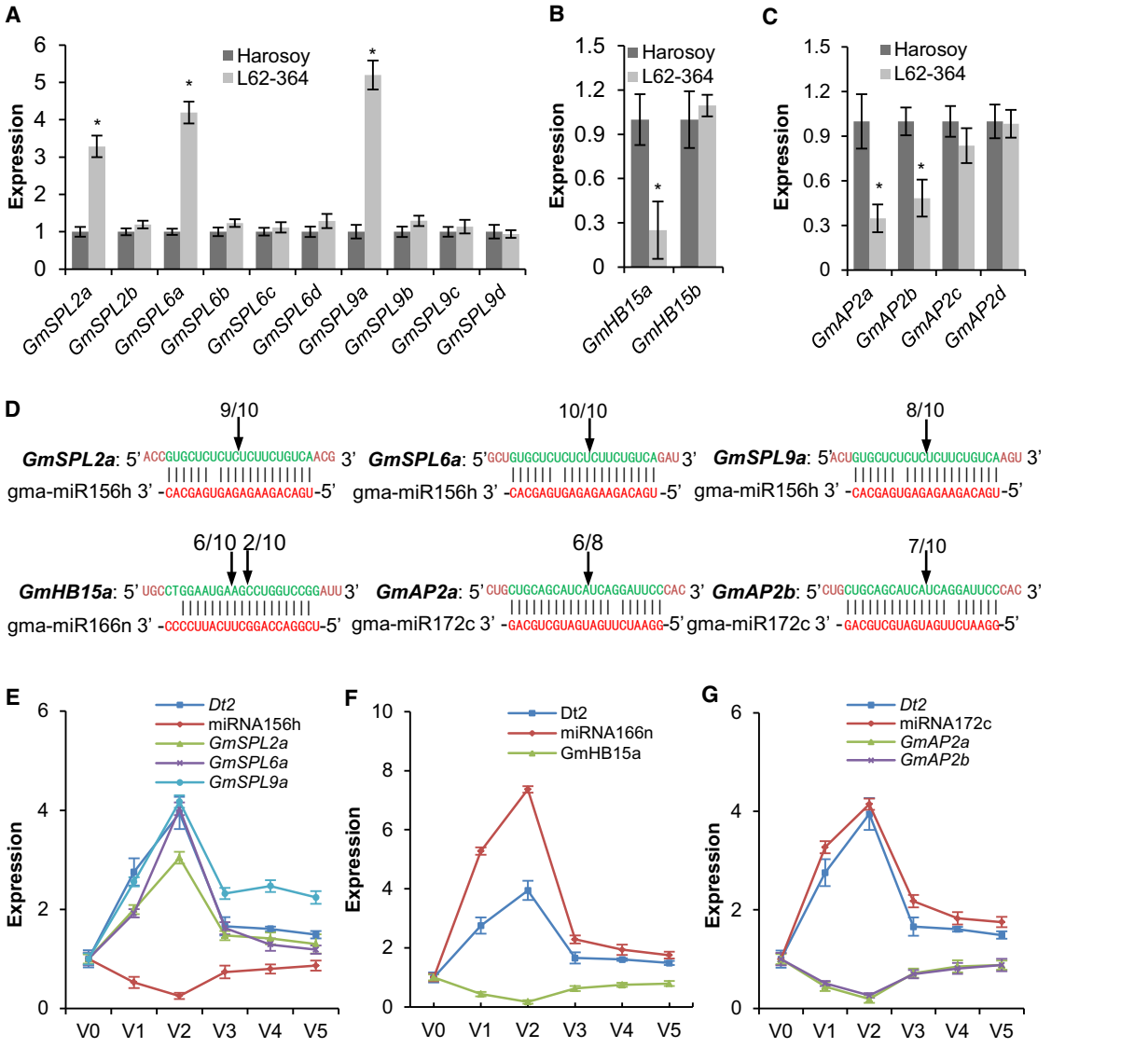

Figure 5. Validation of the miRNA Target Genes by 5′ RACE and Expression Analyses.

(A) The relative expression levels of the predicted miR156h target genes in the stem tips at the V2 stage of Harosoy and L62-364 plants using qRT–PCR. Expression levels are relative to expression of *Cons4* and shown as mean ± SEM from three biological replicates. Asterisks indicate a significant change (*$P < 0.05$, Student's *t*-test).

(B) qRT–PCR analysis of predicted miR166n target gene expression in the stem tips at the V2 stage of Harosoy and L62-364 plants. Expression levels are relative to expression of *Cons4* and shown as mean ± SEM from three biological replicates. Asterisks indicate a significant change (*$P < 0.05$, Student's *t*-test).

(C) qRT–PCR analysis of predicted miR172c target gene expression in the stem tips at the V2 stage of Harosoy and L62-364 plants. Expression levels are relative to expression of *Cons4* and shown as mean ± SEM from three biological replicates. Asterisks indicate a significant change (*$P < 0.05$, Student's *t*-test).

(D) Validation of miR156h, miR166n, and miR172c target genes and cleavage sites using 5′ RACE. Vertical arrows indicate the 5′ termini of the miRNA-guided cleavage products, as identified by 5′ RACE, with the frequency of clones shown.

(E–G) Expression patterns of *Dt2*, miRNA, and miRNA-target genes as indicated. Expression levels of miRNAs and genes in stem tips of L62-364 from the V0 to V5 stages. Values are shown as mean ± SEM from three biological replicates. Expression level of each gene/miRNA at the V0 stage was set as 1, and those at other stages were adjusted accordingly.

See also Supplemental Figures 4 and 5.

Supplemental Table 2) and showed significantly lower levels of expression in the V2-stage stem tip of the *Dt2*-NIL than in that of the *dt2*-NIL (Figure 5B). Expression of all three miRNAs and their targets showed co-expression (either positive or negative association) with *Dt2* in stem tips of L62-364 from developmental stages V0 to V5 (Figure 5E and Supplemental Figure 7). Together, these observations support our hypothesis that the Dt2-modulated miR156h–*GmSPL2a*/*GmSPL6a*/*GmSPL9a* interaction represses the vegetative–reproductive stage transition, the Dt2-modulated miR172c–*GmAP2a*/*GmAP2b* interaction

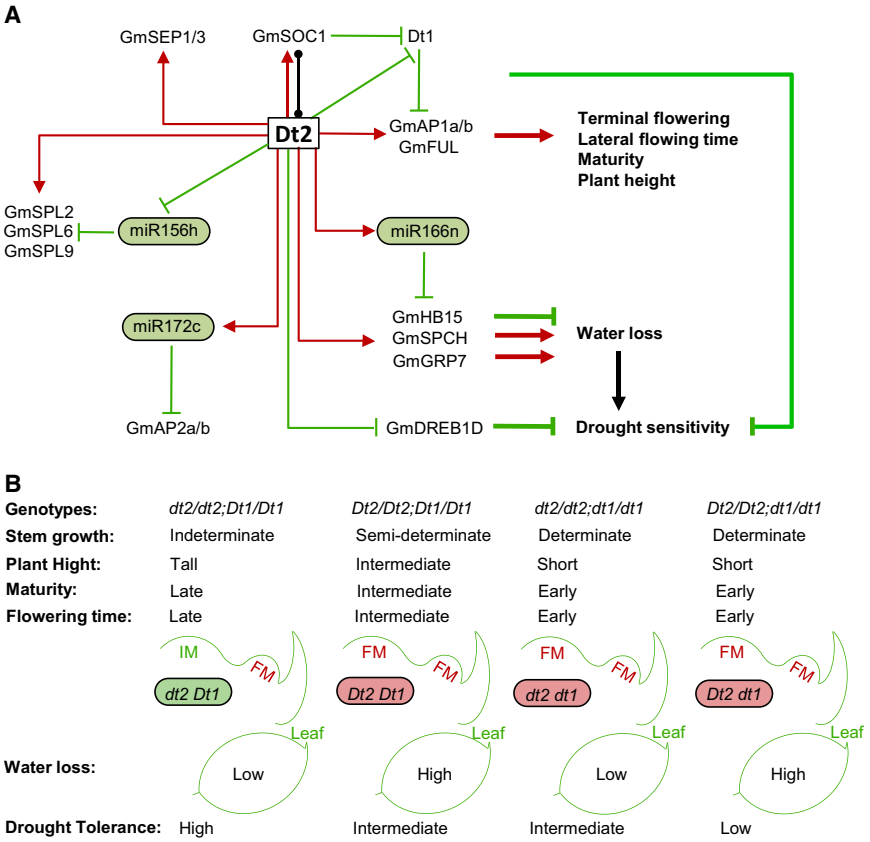

Figure 6. A Model of *Dt2*-Mediated Regulatory Mechanisms Modulating Pleiotropic Traits in Soybean.

(A) *Dt2*-mediated divergent pathways and potential roles in regulating different, similar, and/or relevant traits. Arrows indicate positive regulation, while blunt ends denote negative regulation. Thin arrow lines indicate genetic pathways, while thick arrow lines indicate proposed roles of genetic pathways in modulating agronomic traits.

(B) Phenotypic differences among plants with four distinct genotypes at the *Dt1* and *Dt2* loci.

promotes the vegetative–reproductive stage transition, and the Dt2-modulated miR166n–*GmHB15a* interaction reduces tolerance to drought stress. Other predicted target genes of miR156h, miR172c, and miR166n did not exhibit differential expression between the *Dt2*-NIL and the *dt2*-NIL and between *Dt2*-overexpression lines and the *dt2* control (Supplemental Figure 7), suggesting that these genes may not be targets of these miRNAs.

In addition to these three miRNA families with putative targets directly associated with flowering, stomatal activities, and responses to drought, the other two families of miRNAs bound by Dt2, miR160 and miR167, were predicted to target a number of soybean genes closely related to members of the *Arabidopsis* auxin response factor (ARF) gene family including *ARF6*, *ARF8*, *ARF10*, *ARF16*, and *ARF17* (Supplemental Data 4). Among these family members ARFs, ARF6 and ARF8 were found to regulate JA biosynthesis (Tabata et al., 2010). Hence, the modulation of soybean development and stress responses by Dt2 likely involves hormonal crosstalk.

DISCUSSION

The identification of *Dt2*-mediated genetic pathways provides deeper insight into how this gain-of-function mutation systemically regulates stem growth habit and other traits associated with yield potential and environmental resilience at the molecular level. This information lays the foundation for dissection of additional pathways underlying these traits and will lead to soybean improvement through precise modification of genetic interactions/pathways.

Dt2-Mediated Divergent and Convergent Pathways Unveil Molecular Links between Related and Seemingly Unrelated Pleiotropic Traits

In this study, we identified a set of divergent and convergent pathways mediated by the *Dt2* mutation and elucidated, to a certain extent, the molecular links between stem growth habit and other key traits that determine the plant's overall agronomic performance, including flowering time, maturity, water loss, and tolerance to drought stress (Figure 6A). Because Dt2-modulated semi-determinacy in soybean is distinct from all known mechanisms modulating semi-determinacy in other plants including tomato (Pnueli et al., 1998; Fridman et al., 2002) and the leguminous species pigeon pea (*Cajanus cajan*) (Gupta and Kapoor, 1991) and chickpea (*Cicer arietinum*) (Hegde, 2011), the *Dt2*-mediated divergent pathways that arose after domestication are apparently unique to soybean. Nevertheless, the convergent pathways that affect related traits (e.g., stem growth habit and flowering time) and seemingly unrelated traits (e.g., stem growth habit and stomatal activity) appear to be substantially conserved between soybean and *Arabidopsis* (Bradley et al., 1997; Macalister et al., 2007; Kim et al., 2008; Tian et al., 2010; Figure 6A), particularly when the specificity and difference in spatiotemporal expression of individual pathway genes (i.e., those expressed in apical meristems versus those expressed in lateral meristems) between the two plants are not considered (Figure 6B).

Because Dt2 is an MADS-domain factor that generally functions through the formation of homodimers, heterodimers, or tetramers, the Dt2-mediated regulatory pathways that were recently established in SAMs of semi-determinate soybean (e.g., Dt2–*Dt1*) to promote terminal flowering may indeed be highly similar to those known regulatory pathways (e.g., AP1–*TFL1*) that are expressed in lateral meristems of *Arabidopsis*, although *Dt2* and *GmAP1* are neither functional counterparts nor evolutionarily diverged orthologs (Ping et al., 2014). Since the formation of semi-determinate stems is established by spatiotemporal expression of *Dt2* in SAMs, the pleiotropic effects of Dt2 on other traits such as stomatal activity and water loss can be attributed to

the differential expression of *Dt2*/*dt2* in leaves. Therefore, the pleiotropy of *Dt2* in modulating seemingly unrelated traits appears to be largely determined by the trajectories of spatiotemporal gene expression in different tissues and developmental stages.

Broader effects of Dt2 on soybean plant development, growth, and stress responses are indicated by the Dt2 mediation of molecular pathways involving miRNA and hormonal crosstalk. Although whether the compared homologs/orthologs possess similar functions between soybean and *Arabidopsis* remains to be elucidated, the predicted miRNA-target gene partners in soybean (Supplemental Data 4) are indeed highly conserved with the validated miRNA-target gene partners in *Arabidopsis* (D'Ario et al., 2017; Song et al., 2019) For example, miR160 and miR167 target *ARF* genes and miR156 targets *SPL* genes in both *Arabidopsis* and soybean. If the majority of the detected soybean genes directly and indirectly regulated by Dt2 are indeed functionally conserved, the effects of Dt2 on soybean plant growth and development would be considerably comprehensive.

Enhancement of Agroecological Adaptation and Environmental Resilience of Soybean by Molecular Design

This study was motivated not only by our interest in understanding the molecular bases underlying pleiotropic traits of agronomic importance, but also our intent to pave the way for effective and efficient trait optimization for enhanced environmental resilience and productivity. Soybean varieties with different stem growth habits, an important adaption trait, are grown in different agroecological regions. In general, indeterminate cultivars have more overlap of vegetative growth with reproductive development, providing better adaptation to shorter growing seasons in the northern ecoregions of both the United States and China (Heatherly and Elmore, 2004). By contrast, determinate soybean cultivars have distinctly separate vegetative and reproductive stages, and are relatively late maturing and grown in the south. Semi-determinate cultivars produce stems with terminal racemes similar to those observed in determinate cultivars but show intermediate phenotypes for important agronomic traits such as plant height and node density, and are mainly grown in the north. Because semi-determinate cultivars usually produce slightly fewer stem nodes than indeterminate cultivars, they are somewhat shorter than indeterminate cultivars and thus provide some degree of lodging resistance that is desirable for production in highly fertile and irrigated environments (Chang et al., 1982). Similar to traits controlled by the "green revolution" genes in cereals, this growth habit represents an important target for enhancement of soybean yield potential (Peng et al., 1999; Ping et al., 2014). In fact, semi-determinate cultivars produce even more pods per plant than indeterminate cultivars if they do not lodge (Setiyono et al., 2007). With the availability of *Dt2*- and *Dt1*-based molecular markers (Tian et al., 2010; Ping et al., 2014), it has been very straightforward to convert a soybean variety from one stem growth habit to another.

As demonstrated in this study, both semi-determinate and determinate plants exhibit higher sensitivity to drought stress than indeterminate plants (Figure 3G). Excitingly, this study provides possible solutions for enhancing the WUE and drought stress tolerance of determinate and semi-determinate plants. For example, modifying the Dt2-binding sites in the promoter regions of *GmSPCH* and *GmGRP7* (e.g., by CRISPR/Cas9) would reduce the expression levels of these two genes, resulting in reduction in stomatal density and stomatal aperture for enhanced WUE, whereas modifying the Dt2-binding sites in the promoter region of *GmDREB1D* would result in an increase in the expression level of *GmDREB1D* for improved drought tolerance. If the tolerance of semi-determinate plants to drought stress can be substantially enhanced through these approaches, their potential for grain yield will certainly be boosted in non-irrigated environments.

METHODS

Plant Materials, Growing Conditions, and Genotyping

The four Harosoy NILs, namely Harosoy (*dt2*/*dt2*;*Dt1*/*Dt1*, indeterminate), L62-364 (*Dt2*/*Dt2*;*Dt1*/*Dt1*, semi-determinate), L62-973 (*dt2*/*dt2*;*dt1*/*dt1*, determinate), and L67-3256 (*Dt2*/*Dt2*;*dt1*/*dt1*, determinate), the semi-determinate elite soybean line NE3001 (*Dt2Dt2*;*Dt1Dt1*), and the indeterminate soybean elite line IA3023 (*dt2dt2*;*Dt1Dt1*) were obtained from the USDA Soybean Germplasm Collection. The indeterminate soybean elite line Thorne (*dt2dt2*;*Dt1Dt1*) and the *Dt2*-overexpression transgenic lines (917-55, 917-56, and 917-65) in the Thorne genetic background were previously described (Ping et al., 2014). The seedlings of different genetic backgrounds were grown in the greenhouse at a temperature of 28°C–30°C and a 16-h/8-h day/night cycle.

Western Blot

Total protein samples were extracted from the V2-stage stem tips, the second trifoliate, or seeds with 2× SDS loading buffer. Tissues were lysed with use of a buffer (20 mM Tris [pH 8.0], 1 mM EDTA, 10% glycerin, 0.2% Triton X-100, 1 mM phenylmethylsulfonyl fluoride, and protease inhibitor cocktail [Roche]). Extracted proteins were centrifuged and the suspensions incubated at 95°C for 10 min. Proteins were separated by SDS–PAGE and transferred to polyvinylidene fluoride membranes for immunoblotting.

ChIP and ChIP-Seq

ChIP was performed as described previously (Liu et al., 2016) using stem tips of NE3001 at the V2 stage. In brief, 5 g of stem tips were crosslinked with 1% formaldehyde for 20 min. Nuclei were isolated and the chromatin solution was sonicated for 30 min to shear DNA to a size range of 200–500 bp. Antibody against Dt2 and the IgG (Sigma-Aldrich) control were used for immunoprecipitation. Immune complex was collected by protein G agarose (Millipore 16-266) and DNA was purified by a QIAquick PCR Purification kit (Qiagen 28 106). The ChIPed DNA was prepared for Illumina sequencing using a method similar to one previously described (Lister et al., 2009). The enriched DNA sample was sequenced using an Illumina sequencer to generate pair-ended 100-bp sequence reads.

Analysis of ChIP-Seq Data

Raw reads from ChIP-seq data were aligned to the soybean reference genome (Williams 82, Version 2.0; Phytozome v10) using the Burrows-Wheeler Aligner program (BWA Version 0.7.15-r1140; Li and Durbin, 2010), allowing at most two mismatches. The Sequence Alignment/Map (SAMTools) program (Version 1.3.2, Li et al., 2009) was used for generating BAM files. Peak detection was performed with Model-based Analysis of ChIP-Seq (MACS2) (version 2.1.0.20140616), with the parameters -g 1100000000 –bw 100 (Zhang et al., 2008). Peaks, with a fold change >4.8 and a q value $<10^{-6}$, compared with the mock data, were used for further analysis. To visualize the abundance of selected peaks, we used BEDTools (version v2.26.0-35-g6114307, Quinlan and Hall,

2010) and Integrative Genomics Viewer igvtools (version 2.3.60, Thorvaldsdóttir et al., 2013) to transform the format from BAMs to bedGraph files and normalize the abundance between mock and ChIP data, respectively. To detect the distribution of peaks, we first divided gene-related regions into different feature regions: promoter regions (2-kb region upstream of the TSS for a given gene), gene body regions, and 3′ end regions (2-kb region downstream of the transcription termination site) based on the genome annotation file (gff3, Phytozome 10). Each feature region was then divided into 20 windows and the peak frequency in each window was calculated.

Motif Analysis

To investigate whether the peak sequences bound by Dt2 contain motifs, we extracted the peak sequences using the getFasta function in BEDTools (Quinlan and Hall, 2010). The HOMER program (version 4.7b, Heinz et al., 2010) was used for motif finding and enrichment analysis with the default parameters.

GO Analysis

For the GO enrichment analysis, the GO-term file was reformatted based on the annotated GO list (Phytozome 10) using an in-house Perl script. GO enrichment analysis was used to find which Go terms are over-represented among the set of the Dt2 target genes. GO enrichment was estimated by performing a hypergeometric test using custom R scripts and significance (*P* value) was adjusted by false discovery rate (Benjamini and Hochberg, 1995). GO terms with *q* value < 0.05 were regarded as significantly enriched. The network was visualized using BiNGO (version 3.0.3) and Cytoscape (version 3.4.0).

EMSA

EMSA was performed as described previously (Liu et al., 2016). In brief, the *Dt2* coding region was cloned into the Gateway vector *pET-DEST42* containing a 6× His tag (Thermo Fisher Scientific). The construct was transformed into *Escherichia coli* BL21 (DE3). Cells were grown at 37°C for 5 h and induced by the addition of 1 mM isopropyl β-D-1-thiogalactopyranoside. When the optical density (OD_{600}) of the cultured cells was 0.5–0.9, the fusion protein was purified with nickel–nitrilotriacetic acid agarose (Qiagen, 654 catalog 30210). EMSA was performed according to the kit instructions (Roche, 3353591910).

Transient Assays for Activation Activity *In Vivo*

Activation assays were carried out in protoplasts prepared from 2-week-old soybean seedlings grown under short-day conditions (12-h/12-h day/night cycle). The full-length cDNA of *Dt2* was cloned into the plant binary vector221 (pBI221) driven by the 35S promoter to generate pBI221-Dt2. The reporter plasmids GmDREB1D promoter:LUC, GmSPCH promoter:-LUC, and GmGRP7 promoter:LUC were generated, and a plasmid carrying the GUS gene under the control of the 35S promoter was used as a normalization control (LUC, luciferase; GUS, β-glucuronidase). Values are shown as mean ±standard deviation (SD) of three experimental replicates.

RNA Extraction and qRT–PCR

These experiments were conducted following protocols previously described (Tian et al., 2010; Ping et al., 2014; Liu et al., 2016). qPCR was performed on the Applied Biosystems Step One Plus Real-Time PCR System using SYBR Green PCR Master Mix (Thermo Fisher Scientific). The thermal cycle was 95°C for 5 min, then 40 cycles of 95°C for 30 s, 60°C for 30 s, and 72°C for 1 min. The soybean gene *Cons4* (GenBank: BU578186; Libault et al., 2008) was used as the internal control. The data for the relative expression levels were analyzed by a relative quantitation method (ΔCt). All primers used in this study are listed in Supplemental Table 3.

RNA Library Construction and Deep Sequencing

Total RNA was isolated using TRIzol reagent (Invitrogen) according to the manufacturer's instructions. Total RNA was isolated from Thorne and *Dt2*-overexpression transgenic lines at the V2 stage. The quality of total RNA was determined using a Nanodrop spectrometer (Thermo Fisher Scientific, Wilmington, DE) and 1% formaldehyde gel electrophoresis. Total RNA samples were then sent to the Genomics Center at Purdue University for sequencing, and 101-bp paired-end reads were generated with the Illumina HiScanSQ system.

RNA-Seq Data Analysis

The RNA-seq data analysis was performed as previously described (Qiao et al., 2012; Zhang et al., 2016). Raw reads were aligned to the *G. max* reference genome (Williams 82, Version 2.0; Phytozome 10) using TopHat version 2.0.9 with default parameters. DEGs were identified using Cufflinks version 2.2.1 following the workflow with default parameters (Trapnell et al., 2012). Generation of Venn diagrams and heatmaps was performed using R (version 3.2.2).

Drought-Tolerance Assay

For assessment of drought tolerance, the seedlings of different genetic backgrounds (four plants per genotype in a 2.5 × 2.5-inch plastic container) were grown in the greenhouse at a temperature of 28°C–30°C and a 16-h/8-h day/night cycle for 2 weeks to the V2 stage. Water was withheld for 5 days, at which point all plants were irrigated to saturation. Plants that recovered were defined as having "survived," and survival rate was calculated after recovery for 7 days as the percentage of live seedlings.

Water-Loss Assay

Soybean seedlings (n = 5) at the V2 stage were individually weighed to determine the initial fresh weight. The individual samples were then placed onto filter paper under laboratory conditions and weighed after 600 min. The water-loss rate was calculated as (weight − initial fresh weight)/initial fresh weight.

Phylogenetic Trees

Phylogenetic trees were constructed using amino acid sequences following a protocol described previously (Zhao et al., 2015).

Stem-Loop qRT-PCR

The expression patterns of three mature miRNAs were assayed by stem–loop qRT–PCR. Total RNA isolated from stem tips of Harosoy and L62-362 at the V2 stage was used for the initial reverse transcription reaction. The stem–loop-specific reverse transcription for plant miRNAs was performed as described previously (Chen et al., 2005; Varkonyi-Gasic et al., 2007). Briefly, 6 reverse 3′ end nucleotides of mature miRNA were linked to a self-looped sequence to make up the stem-loop primers; the primers bind to the 3′ portion of miRNA molecules, initiating reverse transcription of the mature miRNA. The reverse transcription product is amplified using a miRNA-specific forward primer excluding the last six nucleotides at the 3′ end of the miRNA. The miRNA-specific quantitative real-time forward primer was used for qRT-PCR. Supplemental Table 3 shows the sequences of stem-loop RT primers and miRNA-specific qRT-PCR primers.

Prediction of miRNA Targets and 5′ RACE Mapping of miRNA Cleavage Sites

Putative targets of miRNA were predicted using psRNATarget (Dai and Zhao, 2011). For the 5′ RACE mapping of miRNA cleavage sites, total RNA was isolated from the stem tip of NE3001 at the V2 stage using TRIzol reagent (Invitrogen). A GeneRacer Kit (Invitrogen) was used to process the total RNA and to map the 5′ termini of the primary transcripts. The cDNA samples were amplified by nested PCR

according to the manufacturer's protocols. The products were ligated into the *pGEM*-T Easy Vector (Promega) and then sequenced.

ACCESSION NUMBERS

Sequence data from this article were submitted to the National Center for Biotechnology Sequence Read Archive (NCBI-SRA) database under the BioProject no. PRJNA492484 and accession nos. SRR7890267, SRR7890268, SRR7890266, and SRR7890265 for the ChIP-seq data, and SRR7890264 and SRR7890263 for the RNA-seq data.

SUPPLEMENTAL INFORMATION

Supplemental Information is available at *Molecular Plant Online*.

FUNDING

This work was supported by the Agriculture and Food Research Initiative competitive grants (#2015-67013-22811 and 2018-67013-27425) of the USDA National Institute of Food and Agriculture.

AUTHOR CONTRIBUTIONS

J.M., D.Z., and X.W. designed the research; D.Z., X.W., S.L., C.W., and M.J.G. performed the research; D.Z., X.W., M.V.M., and J.M. analyzed the data; J.M. wrote the manuscript with input from D.Z., X.W., and M.V.M.

ACKNOWLEDGMENTS

We thank Phillip SanMiguel and Paul Parker at Purdue Genomics Core Facility for generating ChIP-seq data, and the editor and anonymous reviewers for constructive comments that improved the manuscript. No conflict of interest declared.

Received: December 13, 2018
Revised: April 28, 2019
Accepted: May 19, 2019
Published: May 28, 2019

REFERENCES

Aukerman, M.J., and Sakai, H. (2003). Regulation of flowering time and floral organ identity by a MicroRNA and its *APETALA2*-like target genes. Plant Cell **15**:2730–2741.

Benjamini, Y., and Hochberg, Y. (1995). Controlling the false discovery rate: a practical and powerful approach to multiple testing. J. Royal Stat. Soc. B **57**:289–300.

Bernard, R.L. (1972). Two genes affecting stem termination in soybeans. Crop Sci. **12**:235–239.

Bradley, D., Ratcliffe, O., Vincent, C., Carpenter, R., and Coen, E. (1997). Inflorescence commitment and architecture in *Arabidopsis*. Science **275**:80–83.

Chang, J.F., Green, D.E., and Shibles, R. (1982). Yield and agronomic performance of semi-determinate and indeterminate soybean stem types. Crop Sci. **22**:97–101.

Chen, C., Ridzon, D.A., Broomer, A.J., Zhou, Z., Lee, D.H., Nguyen, J.T., Barbisin, M., Xu, N.L., Mahuvakar, V.R., Andersen, M.R., et al. (2005). Real-time quantification of microRNAs by stem-loop RT-PCR. Nucleic Acids Res. **33**:e179.

Cho, L.H., Yoon, J., and An, G. (2017). The control of flowering time by environmental factors. Plant J. **90**:708–719.

Dai, X.B., and Zhao, P.X. (2011). psRNATarget: a plant small RNA target analysis server. Nucleic Acids Res. **39**:W155–W159.

D'Ario, M., Griffiths-Jones, S., and Kim, M. (2017). Small RNAs: big impact on plant development. Trends Plant Sci. **22**:1056–1068.

De Folter, S., and Angenent, G.C. (2006). Trans meets cis in MADS science. Trends Plant Sci. **11**:224–231.

Elkind, Y., Gurnick, A., and Kedar, N. (1991). Genetics of semi-determinate growth habit in tomato. HortScience **26**:1074–1075.

Fornara, F., de Montaigu, A., and Coupland, G. (2010). Snapshot: control of flowering in *Arabidopsis*. Cell **141**:e1–e2.

Fridman, E., Liu, Y.S., Carmel-Goren, L., Gur, A., Shoresh, M., Pleban, T., Eshed, Y., and Zamir, D. (2002). Two tightly linked QTLs modify tomato sugar content via different physiological pathways. Mol. Genet. Genomics **266**:821–826.

Gimenez-Ibanez, S., Boter, M., Ortigosa, A., García-Casado, G., Chini, A., Lewsey, M.G., Ecker, J.R., Ntoukakis, V., and Solano, R. (2017). JAZ2 controls stomata dynamics during bacterial invasion. New Phytol. **213**:1378–1392.

Gupta, S.C., and Kapoor, R.K. (1991). Inheritance of growth habit in pigeonpea. Crop Sci. **31**:1456–1459.

Guttikonda, S.K., Valliyodan, B., Neelakandan, A.K., Tran, L.S., Kumar, R., Quach, T.N., Voothuluru, P., Gutierrez-Gonzalez, J.J., Aldrich, D.L., Pallardy, S.G., et al. (2014). Overexpression of *AtDREB1D* transcription factor improves drought tolerance in soybean. Mol. Biol. Rep. **41**:7995–8008.

Heatherly, L.G., and Elmore, R.W. (2004). Managing inputs for peak production. In Soybeans: Improvement, Production, and Uses, 3rd edn, Agronomy Monograph, *16*, H.R. Boerma and J.E. Specht, eds. (Madison, WI: American Society of Agronomy, Crop Science Society of America, Soil Science Society of America), pp. 451–536.

Hegde, V.S. (2011). Morphology and genetics of a new found determinate genotype in chickpea. Euphytica **182**:35–42.

Heinz, S., Benner, C., Spann, N., Bertolino, E., Lin, Y.C., Laslo, P., Cheng, J.X., Murre, C., Singh, H., and Glass, C.K. (2010). Simple combinations of lineage determining transcription factors prime *cis*-regulatory elements required for macrophage and B cell identities. Mol. Cell **38**:576–589.

Kawagoe, Y., and Murai, N. (1996). A novel basic region/helix-loop-helix protein binds to a G-box motif CACGTG of the bean seed storage protein β-phaseolin gene. Plant Sci. **116**:47–57.

Kidner, C.A., and Martienssen, R.A. (2005). The developmental role of microRNA in plants. Curr. Opin. Plant Biol. **8**:38–44.

Kim, J.S., Jung, H.J., Lee, H.J., Kim, K.A., Goh, C.H., Woo, Y., Oh, S.H., Han, Y.S., and Kang, H. (2008). Glycine-rich RNA-binding protein 7 affects abiotic stress responses by regulating stomata opening and closing in *Arabidopsis thaliana*. Plant J. **55**:455–466.

Kuroda, T., Saitoh, K., Mahmood, T., and Yanagawa, K. (1998). Differences in flowering habit between determinate and indeterminate types of soybean. Plant Prod. Sci. **1**:18–24.

Lata, C., and Prasad, M. (2011). Role of *DREB*s in regulation of abiotic stress responses in plants. J. Exp. Bot. **62**:4731–4748.

Li, H., and Durbin, R. (2010). Fast and accurate long-read alignment with Burrows-Wheeler transform. Bioinformatics **26**:589–595.

Li, H., Handsaker, B., Wysoker, A., Fennell, T., Ruan, J., Homer, N., Marth, G., Abecasis, G., and Durbin, R.; 1000 Genome Project Data Processing Subgroup (2009). The Sequence alignment/map (SAM) format and SAMtools. Bioinformatics **25**:2078–2079.

Libault, M., Thibivilliers, S., Bilgin, D.D., Radwan, O., Benitez, M., Clough, S.J., and Stacey, G. (2008). Identification of four soybean reference genes for gene expression normalization. Plant Genome **1**:44–54.

Lister, R., Pelizzola, M., Dowen, R.H., Hawkins, R.D., Hon, G., Tonti-Filippini, J., Nery, J.R., Lee, L., Ye, Z., Ngo, Q.M., et al. (2009). Human DNA methylomes at base resolution show widespread epigenomic differences. Nature **462**:315–322.

Liu, B., Fujita, T., Yan, Z.H., Sakamoto, S., Xu, D., and Abe, J. (2007). QTL mapping of domestication-related traits in soybean (*Glycine max*). Ann. Bot. **100**:1027–1038.

Liu, B., Watanabe, S., Uchiyama, T., Kong, F., Kanazawa, A., Xia, Z., Nagamatsu, A., Arai, M., Yamada, T., Kitamura, K., et al. (2010). The soybean stem growth habit gene *Dt1* is an ortholog of *Arabidopsis TERMINAL FLOWER1*. Plant Physiol. **153**:198–210.

Liu, C., Thong, Z.H., and Yu, H. (2009). Coming into bloom: the specification of floral meristems. Development **136**:3379–3391.

Liu, Y., Zhang, D., Ping, J., Li, S., Chen, Z., and Ma, J. (2016). Innovation of a regulatory mechanism modulating semi-determinate stem growth through artificial selection in soybean. PLoS Genet. **12**:e1005818.

Macalister, C.A., Ohashi-Ito, K., and Bergmann, D.C. (2007). Transcription factor control of asymmetric cell divisions that establish the stomatal lineage. Nature **445**:537–540.

Marcos, A.D., Houbaert, A., Triviño, M., Delgado, D., Martíntrillo, M., Russinova, E., Fenoll, C., and Mena, M. (2017). A mutation in the bHLH domain of the SPCH transcription factor uncovers a BR-dependent mechanism for stomatal development. Plant Physiol. **174**:823–842.

Melzer, S., Lens, F., Gennen, J., Vanneste, S., Rohde, A., and Beeckman, T. (2008). Flowering-time genes modulate meristem determinacy and growth form in *Arabidopsis thaliana*. Nat. Genet. **40**:1489–1492.

O'Maoiléidigh, D.S., Graciet, E., and Wellmer, F. (2014). Gene networks controlling *Arabidopsis thaliana* flower development. New Phytol. **201**:16–30.

Peng, J., Richards, D.E., Hartley, N.M., Murphy, G.P., Devos, K.M., Flintham, J.E., Beales, J., Fish, L.J., Worland, A.J., Pelica, F., et al. (1999). 'Green revolution' genes encode mutant gibberellin response modulators. Nature **400**:256–261.

Ping, J., Liu, Y., Sun, L., Zhao, M., Lin, F., Sui, Y., She, M., Nelson, R.L., Clemente, T., Specht, J., et al. (2014). *Dt2* is an *APETALA1*-like MADS-domain factor gene that controls semi-determinacy in soybean. Plant Cell **26**:2831–2842.

Pnueli, L., Carmel-Goren, L., Hareven, D., Gutfinger, T., Alvarez, J., Ganal, M., Zamir, D., and Lifschitz, E. (1998). The SELF-PRUNING gene of tomato regulates vegetative to reproductive switching of sympodial meristems and is the ortholog of *CEN* and *TFL1*. Development **125**:1979–1989.

Qiao, H., Shen, Z., Huang, S.S.C., Schmitz, R.J., Urich, M.A., Briggs, S.P., and Ecker, J.R. (2012). Processing and subcellular trafficking of ER-tethered EIN2 control response to ethylene gas. Science **338**:390–393.

Quinlan, A.R., and Hall, I.M. (2010). BEDTools: a flexible suite of utilities for comparing genomic features. Bioinformatics **26**:841–842.

Schmid, M., Uhlenhaut, N.H., Godard, F., Demar, M., Bressan, R., Weigel, D., and Lohmann, J.U. (2003). Dissection of floral induction pathways using global expression analysis. Development **130**:6001–6012.

Schmutz, J., Cannon, S.B., Schlueter, J., Ma, J., Mitros, T., Nelson, W., Hyten, D.L., Song, Q., Thelen, J.J., Cheng, J., et al. (2010). Genome sequence of the palaeopolyploid soybean. Nature **463**:178–183.

Schomburg, F.M., Bizzell, C.M., Lee, D.J., Zeevaart, J., and Amasino, R.M. (2003). Overexpression of a novel class of gibberellin 2-oxidases decreases gibberellin levels and creates dwarf plants. Plant Cell **15**:151–163.

Setiyono, T.D., Weiss, A., Specht, J., Bastidas, A.M., Cassman, K.G., and Dobermann, A. (2007). Understanding and modeling the effect of temperature and day length on soybean phenology under high-yield conditions. Field Crops Res **100**:257–271.

Shore, P., and Sharrocks, A.D. (1995). The MADS-box family of transcription factors. Eur. J. Biochem. **229**:1–13.

Simon, R., Igeño, M.I., and Coupland, G. (1996). Activation of floral meristem identity genes in *Arabidopsis*. Nature **384**:59–62.

Smaczniak, C., Immink, R.G., Angenent, G.C., and Kaufmann, K. (2012). Developmental and evolutionary diversity of plant MADS-domain factors: insights from recent studies. Development **139**:3081–3098.

Song, X., Li, Y., Cao, X., and Qi, Y. (2019). MicroRNAs and their regulatory roles in plant-environment interactions. Annu. Rev. Plant Biol. **70**:489–525.

Spanudakis, E., and Jackson, S. (2014). The role of microRNAs in the control of flowering time. J. Exp. Bot. **65**:365–380.

Specht, J.E., Chase, K., Macrander, M., Graef, G.L., Chung, J., Markwell, J.P., Germann, M., Orf, J.H., and Lark, K.G. (2001). Soybean response to water: a QTL analysis of drought tolerance. Crop Sci. **41**:493–509.

Tabata, R., Ikezaki, M., Fujibe, T., Aida, M., Tian, C.E., Ueno, Y., and Ishiguro, S. (2010). Arabidopsisauxin response factor6 and 8 regulate jasmonic acid biosynthesis and floral organ development via repression of class 1 KNOX genes. Plant Cell Physiol **51**:164–175.

Tanaka, Y., and Shiraiwa, T. (2009). Stem growth habit affects leaf morphology and gas exchange traits in soybean. Ann. Bot. **104**:1293–1299.

Teotia, S., and Tang, G. (2015). To bloom or not to bloom: role of microRNAs in plant flowering. Mol. Plant **8**:359–377.

Thorvaldsdóttir, H., Robinson, J.T., and Mesirov, J.P. (2013). Integrative Genomics Viewer (IGV): high-performance genomics data visualization and exploration. Brief. Bioinform. **14**:178–192.

Tian, Z., Wang, X., Lee, R., Li, Y., Specht, J., Nelson, R., McClean, P., Qiu, L., and Ma, J. (2010). Artificial selection for determinate growth habit in soybean. Proc. Natl. Acad. Sci. U S A **107**:8563–8568.

Trapnell, C., Roberts, A., Goff, L., Pertea, G., Kim, D., Kelley, D.R., Pimentel, H., Salzberg, S.L., Rinn, J.L., and Pachter, L. (2012). Differential gene and transcript expression analysis of RNA-seq experiments with TopHat and Cufflinks. Nat. Protoc. **7**:562–578.

Varkonyi-Gasic, E., Wu, R., Wood, M., Walton, E.F., and Hellens, R.P. (2007). Protocol: a highly sensitive RT-PCR method for detection and quantification of microRNAs. Plant Methods **3**:1746–1748.

Vicente, M.H., Zsögön, A., Sá, A.F.L., Ribeiro, R.V., and Peres, L.E.P. (2015). Semi-determinate growth habit adjusts the vegetative-to-reproductive balance and increases productivity and water-use efficiency in tomato (*Solanum lycopersicum*). J. Plant Physiol. **177**:11–19.

Wong, C.E., Singh, M.B., and Bhalla, P.L. (2009). Molecular processes underlying the floral transition in the soybean shoot apical meristem. Plant J. **57**:832–845.

Xu, M., Hu, T., Zhao, J., Park, M.Y., Earley, K.W., Wu, G., Yang, L., and Poethig, R.S. (2016). Developmental functions of miR156-regulated *SQUAMOSA PROMOTER BINDING PROTEIN-LIKE* (*SPL*) genes in *Arabidopsis thaliana*. PLoS Genet. **12**:e1006263.

Yant, L., Mathieu, J., and Schmid, M. (2009). Just say no: floral repressors help *Arabidopsis* bide the time. Curr. Opin. Plant Biol. **12**:580–586.

Zhai, Q., Zhang, X., Wu, F., Feng, H., Deng, L., Xu, L., Zhang, M., Wang, Q., and Li, C. (2015). Transcriptional mechanism of jasmonate receptor COI1-mediated delay of flowering time in *Arabidopsis*. Plant Cell **27**:2814–2828.

Zhang, F., Qi, B., Wang, L., Zhao, B., Rode, S., Riggan, N.D., Ecker, J.R., and Qiao, H. (2016). EIN2-dependent regulation of acetylation of histone H3K14 and non-canonical histone H3K23 in ethylene signalling. Nat. Commun. **7**:13018.

Zhang, J., Zhang, H., Srivastava, A.K., Pan, Y., Bai, J., Fang, J., Shi, H., and Zhu, J.K. (2018). Knockdown of rice microRNA166 confers drought resistance by causing leaf rolling and altering stem xylem development. Plant Physiol. **176**:2082–2094.

Zhang, Y., Liu, T., Meyer, C.A., Eeckhoute, J., Johnson, D.S., Bernstein, B.E., Nussbaum, C., Myers, R.M., Brown, M., Li, W., et al. (2008). Model-based analysis of ChIP-seq (MACS). Genome Biol. **9**:R137.

Zhao, M., Meyers, B.C., Cai, C., Xu, W., and Ma, J. (2015). Evolutionary patterns and co-evolutionary consequences of MIRNA genes and microRNA targets triggered by multiple mechanisms of genomic duplications in soybean. Plant Cell **27**:546–562.